Molecular Dynamics Simulations of Asialoglycoprotein Receptor Ligands

P. V. Balaji, P. K. Qasba,* and V. S. R. Rao

Laboratory of Mathematical Biology, National Cancer Institute, National Institutes of Health, Building Park 5, Room 410, 9000 Rockville Pike, Bethesda, Maryland 20892

Received June 24, 1993; Revised Manuscript Received September 9, 1993®

ABSTRACT: Several recent studies have implicated carbohydrates in cell adhesion, inflammation, clearance of glycoproteins from blood circulation, embryonic development, and metastasis among others. Understanding the conformation of these carbohydrate recognition elements and their interaction at the molecular level is essential for the design of oligosaccharide inhibitors/drugs. Given the difficulty in solving carbohydrate structures by X-ray crystallography and since NMR experiments give only time-averaged conformation, molecular dynamics simulations are well suited to determine all the accessible conformations of oligosaccharides. Present communication reports the simulation of some of the oligosaccharide ligands of asialoglycoprotein receptor for 1 ns using Biosym's InsightII molecular modeling package on NCI-FCRDC's Y-MP 8D/8128 supercomputer. Results obtained from these simulations, in addition to explaining the observed differences in the binding affinities of these ligands to the asialoglycoprotein receptor, have led to a modified model for the recognition of the oligosaccharides by the receptor. Accordingly, only the two terminal galactose residues on the 1,3-arm of the triantennary oligosaccharide ($GlcNAc_2Man_3$ core of the N-linked oligosaccharides with *N*-acetyllactosamine in β1,2- and β1,4-linkages on the 1,3-linked core mannose) are primarily required for recognition, and the terminal galactose on the 1,6-arm (*N*-acetyllactosamine in β1,2-linkage on the 1,6-linked core mannose) provides additional binding energy. It has been shown that the oligosaccharides studied here have significant flexibility and the flexibility is more around the 1,3-linkage than the 1,6-linkage. The need for simulation for longer periods and with multiple initial conformations is also discussed in the present report.

Alternative isomeric linkages between sugars which are generated with the help of specific glycosyltransferases from a relatively small number of saccharide units produce diverse oligosaccharide structures that are present in animal tissues (Roseman, 1970; Satyanarayana & Rao, 1971, 1972; Rao & Satyanarayana, 1973). These complex carbohydrate structures have an enormous potential for encoding information. This information content is further increased by the existence of several conformers for a given oligosaccharide which have been implicated in several biological functions. Among them is their recognition by the cellular membrane receptors involving protein–carbohydrate interactions that leads either to intercellular contacts (Brandley *et al.*, 1990) or to endocytosis of the glycoconjugates by the cell (Ashwell & Harford, 1982).

In solution several conformers of an oligosaccharide exist in equilibrium. As a result, most of the experimental studies in solution give a time-averaged conformation, and this need not be the bioactive conformer. To have a precise idea about the bioactive conformer, it is essential to have information about all the conformers which are accessible by this particular oligosaccharide. Molecular dynamics (MD) simulations of oligosaccharides are being used more often to resolve many questions of direct biological relevance (French & Brady, 1990; Brady, 1991; Tvaroska, 1991). In this study, the molecular dynamics technique has been applied to study all the possible conformations of some of the ligands of asialoglycoprotein receptor (ASGP-R), an important cell surface receptor.

ASGP-R is present on the sinusoidal (blood-facing) surface of hepatocyte plasma membranes and binds terminal galactose (Gal) or *N*-acetylgalactosamine residues of glycoproteins circulating in blood. The binding triggers the endocytosis of the receptor-bound asialoglycoprotein, resulting in the clearance of the glycoprotein from blood circulation. ASGP-R is a heterooligomeric protein consisting of two very similar protomers (Spiess, 1990). These two protomers are transmembrane proteins with the carbohydrate binding domain at their carboxyl terminus. Both the protomers can independently associate to form aggregates which show Gal binding activity. However, there is an absolute requirement of both the protomers for ASGP-R activity. Ligand binding studies showed that the affinity of the ligands to ASGP-R increases exponentially depending on the presence of one, two, or three terminal Gal residues (Lee *et al.*, 1983). Presence of four or more Gal residues showed only marginal or no increase in the binding affinity. A triantennary glycopeptide of *N*-acetyllactosamine type, oligosaccharide **IV** (Chart I), was found to have the highest affinity to ASGP-R (Lee, 1991). The three-dimensional structure of neither the triantennary oligosaccharide nor the two protomers constituting ASGP-R has been determined so far. Hence, the possible modes of binding and consequently the mechanism of recognition of the triantennary oligosaccharides of glycoproteins by ASGP-R have not been delineated.

NMR, fluorescence, and energy minimization techniques have been used earlier to propose a model for the binding of oligosaccharides to ASGP-R. From photoaffinity labeling experiments, it was suggested that Gal9 and Gal11 of oligosaccharide **IV** (Figure 1b) bind to protomer I and Gal10 binds to protomer II of ASGP-R (Rice *et al.*, 1990). From spectroscopic studies and HSEA (hard sphere with exoanomeric effect) calculations on certain bi- and triantennary oligosaccharides, it was proposed that the binding to ASGP-R requires these three Gal residues (i.e., Gal9, Gal10, and Gal11) in a precise geometric arrangement and that the three Gal binding sites of ASGP-R form the vertices of a "golden" triangle (Lee *et al.*, 1984). The two biantennary pentasaccharides, **I** and **II** (Chart I), both of which have two terminal

* Abstract published in *Advance ACS Abstracts,* November 1, 1993.

Chart I: Structures of Oligosaccharides Studied by Molecular Dynamics Simulations in the Present Study[a]

Oligosaccharide	Id #
Gal-β1,4-GlcNAc-(β1,6)-Man Gal-β1,4-GlcNAc-β1,2	I
Gal-β1,4-GlcNAc-(β1,4)-Man Gal-β1,4-GlcNAc-β1,2	II
Gal-β1,4-GlcNAc-β1,2-Man-α1,6 Man Gal-β1,4-GlcNAc-β1,4-Man-α1,3 Gal-β1,4-GlcNAc-β1,2	III
Gal-β1,4-GlcNAc-β1,2-Man-α1,6 Man-β1,4-Chitobiose Gal-(β1,4)-GlcNAc-β1,4-Man-α1,3 Gal-β1,4-GlcNAc-β1,2	IV

[a] Identification numbers are used throughout to refer to these molecules.

Gal residues, show a large variation in their affinity to ASGP-R (Lee *et al.*, 1983; Lodish, 1991) and this could not be explained by the golden triangle model. The variation in the affinity of the two triantennary oligosaccharides which differ in the linkage of the terminal Gal residue (Townsend *et al.*, 1986) also cannot be explained by the golden triangle model.

Molecular dynamics simulations have been performed to study the accessible conformations of the oligosaccharide ligands of ASGP-R. Most of the earlier studies on the conformational behavior of oligosaccharides were limited to the study of individual di- and trisaccharide fragments which constitute the actual oligosaccharides present on glycoproteins. Simulation of the molecules for 1000 ps by considering all the monosaccharides simultaneously has provided a wealth of information about the conformational preferences of these molecules. These data have been used to explain the differences in the binding affinities of the oligosaccharide ligands to ASGP-R. Together with the earlier experimental data from other laboratories (Lee, 1989; Lodish, 1991), results from the present study have led to a modified model for the binding of the triantennary oligosaccharide moieties of glycoproteins to ASGP-R.

METHODS

Oligosaccharides studied in the present work are shown in Chart I. Standard nomenclature was used for naming the atoms and is as shown in Figure 1a. The numbering of the residues and the intersaccharide torsion angles for the oligosaccharides studied are shown schematically in Figure 1b. The torsion angles ϕ,ψ (and χ in 1,6-linkages) have been identified by the residue number of the reducing monosaccharide unit involved in the disaccharide linkage.

Initial Geometry. All the saccharides are D isomers and were considered to be in the $^4C_1$ chair conformation (Stoddart, 1971). Bond lengths and bond angles were taken from the data compiled by X-ray crystallographic analysis (Arnott & Scott, 1972). The bond angle at the glycosidic oxygen was fixed at 117.5°. The 2-acetamido group was fixed using Pauling–Corey geometry (Corey & Pauling, 1953) with the amide bond in a trans conformation. For generating the initial coordinates, the torsion angles for the various interglycosidic bonds were taken from the energy minimization studies (Biswas *et al.*, 1987).

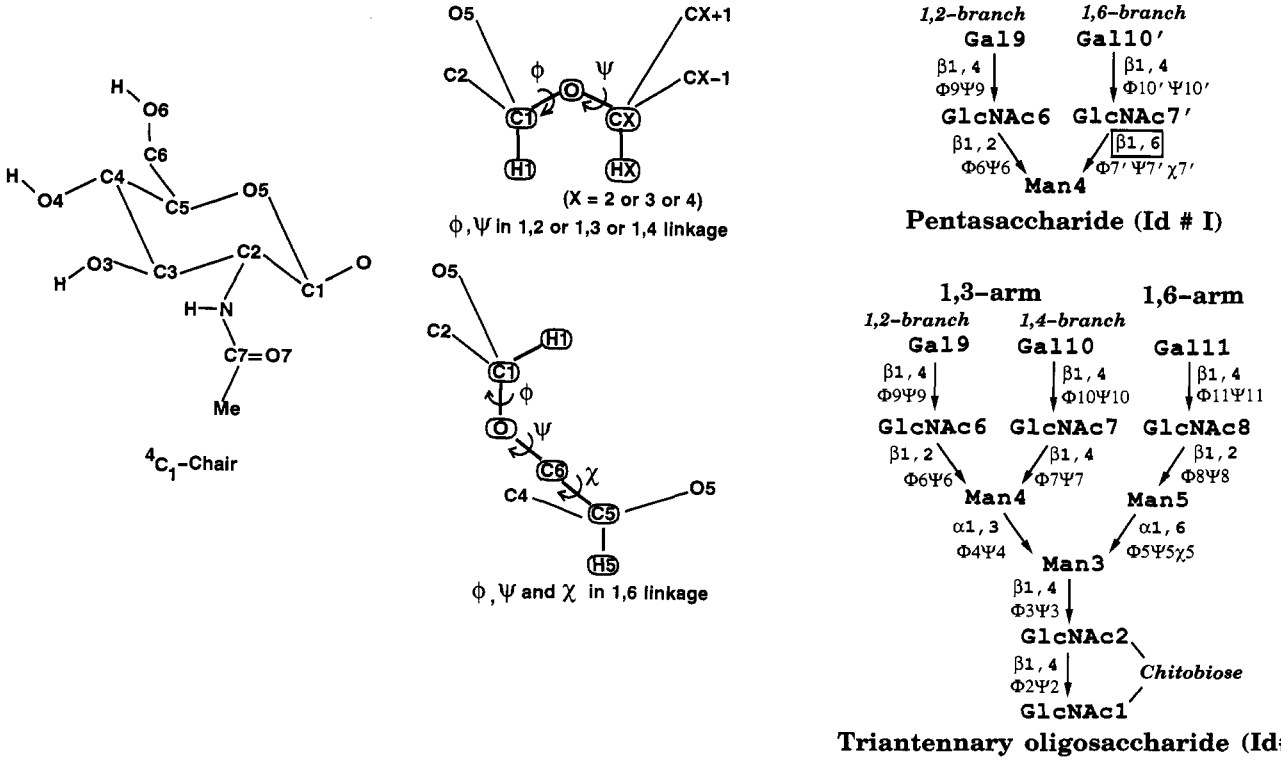

FIGURE 1: (a, left) Atom names and torsion angle definition used in the present study. (b, right) Schematic diagram showing the saccharide numbers and torsion angle names. The trisaccharide fragment Man5-GlcNAc8-Gal11 of the triantennary oligosaccharide IV is referred to as the 1,6-arm, and the pentasaccharide fragment consisting of Man4 and the 1,2- and 1,4-branch *N*-acetyllactosamines is referred to as the 1,3-arm. Since oligosaccharides II and III (Chart I) are part of IV, the same residue and torsion angle numbering scheme is used for all the three oligosaccharides. Residue and torsion angle names in the β1,6-branch of pentasaccharide I are primed to distinguish them from those on the β1,4-branch in oligosaccharides II, III, and IV.

Generation of Coordinates. The coordinates for all the oligosaccharides were generated using the in-house software package IMPAC (*i*nteractive *m*odeling *pac*kage for *c*arbohydrates) developed by P. Sailaja, P. V. Balaji, B. Vijaya Sai Reddy and V. S. R. Rao at the Molecular Biophysics Unit, Indian Institute of Science, Bangalore.

Definition of Torsion Angles. ϕ was considered to be 0° when the H1–C1 bond eclipses the O–CX bond and ψ as 0° when the C1–O bond eclipses the CX–HX bond, where X is 2 or 3 or 4 depending on the linkage type, i.e., 1,2- or 1,3- or 1,4-linkage. In the case of the 1,6-linkage, the three angles, ϕ, ψ, and χ, were defined as H1–C1–O–C6, C1–O–C6–C5, and O–C6–C5–H5 and were taken to be 0° when the first and fourth atoms are cis to each other. These are shown schematically in Figure 1a. A clockwise rotation was considered to be positive.

Calculation Procedure. All calculations were performed using Biosym's InsightII (version 2.1.2; Discover version 2.8) on National Cancer Institute's Cray Y-MP 8D/8128 supercomputer. The initial coordinates obtained from IMPAC were first minimized by the Newton–Raphson algorithm until the maximum derivative is less than 0.001 kcal/Å. This was followed by an equilibration period of 40 ps and a productive run of 1000 ps (=1 ns) at a temperature of 300 K. The average temperature in all the simulations was maintained at 300 K with a standard deviation of up to ±11° in various simulations. A time step of 1 fs (1000 fs = 1 ps) was used for integration which was done using Verlet's leap frog algorithm. Coordinate information was stored for every 100 steps, and only the trajectory data from the productive run (10 000 data points) were considered for analysis. All plots were drawn using the Analysis module of InsightII. The distance between the terminal monosaccharide residues was calculated as the distance between the centers of the respective pyranose rings. The center of the pyranose ring was defined as the arithmetic mean of the four atoms, C2, C3, C5, and O5 (atoms defining the plane of the $^4C_1$ chair), constituting the pyranose ring. A hydrogen bond was considered to be possible only when the distance between the donor and the acceptor atoms is less than or equal to 3.4 Å.

Force Field. The total potential energy of the molecule was calculated by adding the contributions from bond stretching, bond angle bending, torsional strain, van der Waals, and electrostatic components. Bond lengths and bond angles were restrained to their equilibrium values by the use of a harmonic potential function. Torsional strain was calculated using the standard cosine function. van der Waals interactions were evaluated by a Lennard-Jones 6–12 potential function, and electrostatic interactions were calculated using Coulomb's law. No explicit hydrogen-bonding term was included in the calculations. This prevented the formation of unrealistic intra- and intersaccharide hydrogen bonds in the absence of explicit water molecules. Interactions between all the nonbonded atom pairs were calculated without using any distance cutoffs. The default CVFF force field of Discover was used in all calculations.

Given the number and size of the oligosaccharides studied and the length of time for which the molecule has been simulated (1040 ps), it is nearly impossible with the present resources to include explicit water molecules. MD simulations of glucose, *N*-acetylglucosamine, chitobiose, and sialic acid using Biosym's InsightII package with and without explicit inclusion of water molecules for 80 ps showed that the movement of the pendant hydroxyl groups is highly dampened and the hydroxyl hydrogens are restricted to mainly staggered conformations (Mohan, 1993). In order to determine the effect of including solvent molecules in simulations on the conformational behavior of carbohydrates, simulations of Man-α1,3-Man-β1,4-GlcNAc and Man-α1,2-Man have been carried out for 30 ps (Homans, 1990) and 500 ps (Edge *et al.*, 1990), respectively. These studies have shown that explicitly considering solvent molecules in the simulations does not significantly affect the conformational transitions but will only dampen the torsional fluctuations. Hence the effect of water molecules has been indirectly modeled by use of a distance-dependent dielectric constant (4.0*r*) which weighs short-range interactions more than the long-range interactions.

RESULTS

Molecular dynamics simulations of two biantennary (**I** and **II**) and two triantennary oligosaccharides (**III** and **IV**; Chart I) have been carried out for 1000 ps (1 ns). Theoretically, during molecular dynamics simulations, the molecule should sample all the available conformational space. But this is not always the case either due to the shorter simulation period (relative to the time scale of the conformational transition) or due to the very high energy barrier between two conformations. Hence, in the present work, simulations were carried out with three different initial conformations (60°, 180°, and –60°) for χ5 and χ7′. For rotations around other bonds, it was found that a single initial conformation is sufficient since, during the 1000-ps simulation period, the conformational space was well sampled. These results show significant fluctuations in some of the torsion angles besides χ, revealing significant conformational flexibility in these oligosaccharides. This is contrary to earlier assumptions that these complex carbohydrates have rigid conformations.

Simulation of Biantennary Pentasaccharide **I.** Molecular dynamics simulations of pentasaccharide **I** were done with three different starting values for χ7′ (60°, 180°, and –60°). The conformation of the molecule was very similar in all three simulations except around the β1,6-linkage. In the simulations started with χ7′ = 180° and –60°, χ7′ did not show any transitions; i.e., it remained around 180° and –60°, respectively. However, when the simulations were started with χ7′ = 60°, χ7′ changed to –60° during minimization and equilibration period itself and did not go back to 60° during the entire 1000 ps of simulation (Figure 2b). This shows that χ7′ = 60° is energetically less favorable. After about 560 ps, χ7′ changes from –60° to 180°. Such a change in χ7′ brings about significant changes in ϕ7′ and ψ7′. These transitions lead to a totally different conformation for the molecule, as reflected in the distance between Gal9 and Gal10′ (Figure 2d).

Overall, the molecule seems to fluctuate around two distinct conformations: one extended and the second folded, depending on whether χ7′ is around –60° or 180°. Figure 2b shows that the change in χ7′ from –60° to 180° dampens ψ7′ and hence the movement of the 1,6-branch. ϕ6,ψ6 which determine the conformation around the β1,2-linkage do not show any large deviations (Figure 2a) and have average values of 26°, 3°. This leads to an intramolecular hydrogen bond between Man4–O3 and GlcNAc6–O5. ϕ9,ψ9 and ϕ10′,ψ10′ which determine the conformation of the *N*-acetyllactosamine groups have average values of 43°, –9° and 40°, –11°, respectively. These studies also show that one of the terminal Gal residues accesses a conformation around ϕ = 170° for a short duration around 700 ps (Figure 2c). The ϕ,ψ values obtained here for both the β1,2- and β1,4-linkages are in good agreement with the values predicted from earlier force-field calculations for the respective disaccharides (Satyanarayana & Rao, 1971; Imberty *et al.*, 1991). Depending on χ7′, the two Gal residues

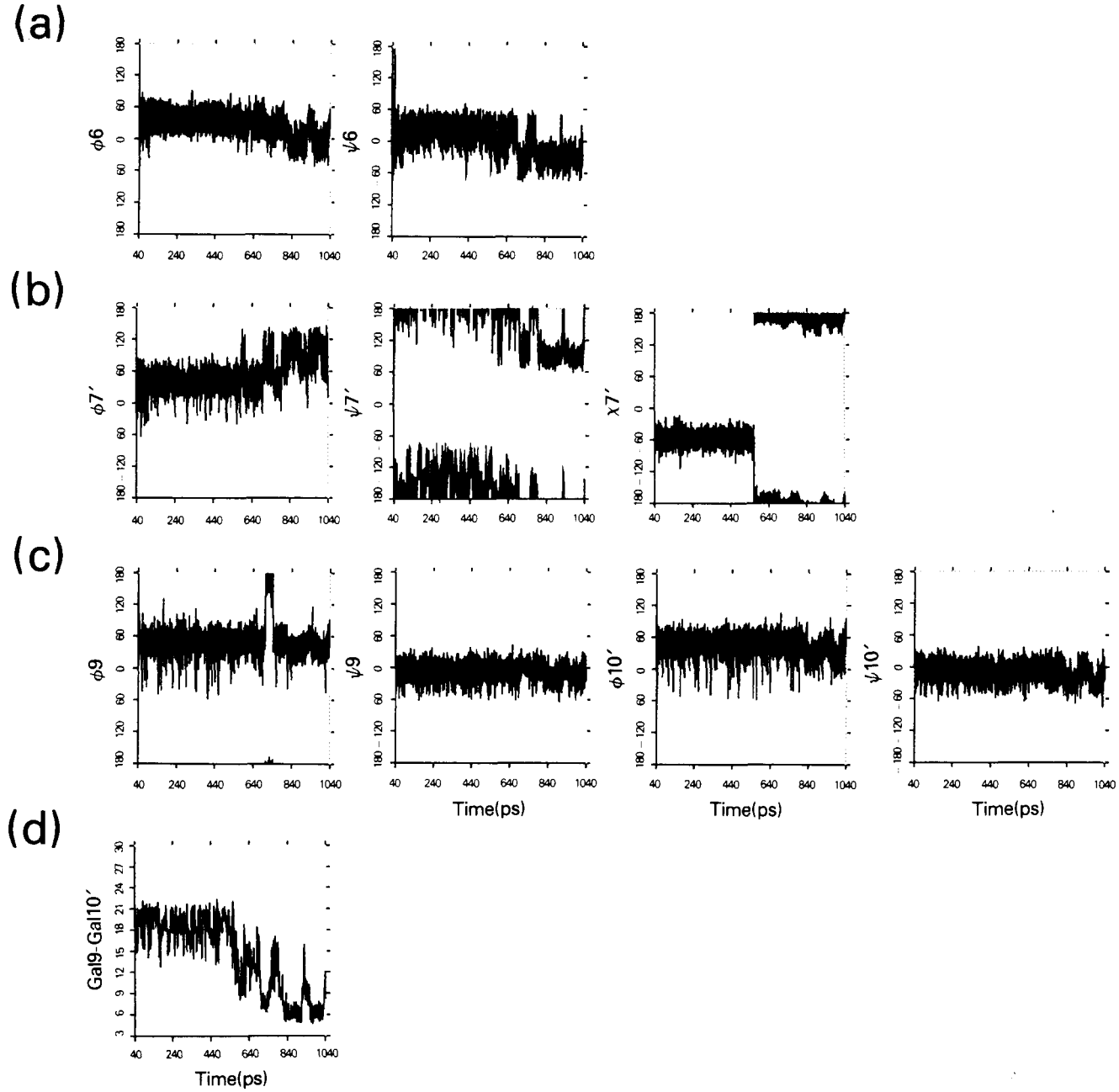

FIGURE 2: Variation of the intersaccharide torsion angles during the course of simulation in pentasaccharide I (initial $\chi 7' = 60°$): (a) $\phi 6,\psi 6$ for GlcNAc6-β1,2-Man4; (b) $\phi 7',\psi 7',\chi 7'$ for GlcNAc7′-β1,6-Man4; (c) $\phi 9,\psi 9$ for Gal9-β1,4-GlcNAc6 and $\phi 10',\psi 10'$ for Gal10′-β1,4-GlcNAc7′; (d) variation in the distance between Gal9 and Gal10′.

will be separated by an average distance of 18.6Å in the extended conformation ($\chi 7' = -60°$) and 9.6Å in the folded conformation ($\chi 7' = 180°$).

Simulation of Biantennary Pentasaccharide **II.** The torsion angle versus time plots for the biantennary pentasaccharide **II** are shown in Figure 3. Pentasaccharide **II** differs from **I** in having a β1,4-linkage instead of β1,6 between GlcNAc7′ and Man4 (Chart I; Figure 1b). The conformation of the *N*-acetyllactosamine moieties (Gal9-β1,4-GlcNAc6 and Gal10-β1,4-GlcNAc7) in pentasaccharide **II** is very similar to that seen in **I**. The average values of $\phi 9,\psi 9$ and $\phi 10,\psi 10$ which define the conformation of the terminal Gal residue are 44°, −8° and 44°, −6°, respectively. Fluctuations in $\phi 9$ and $\phi 10$ seem to be large compared to those in the corresponding ψ values (Figure 3c). Occasionally, $\phi 9$ and $\phi 10$ change to around 180° during the MD simulations, leading to a flipping of the Gal residues. $\phi 7,\psi 7$ which determine the conformation of the GlcNAc7-β1,4-Man4 fragment have an average value of 53°, −5°, in good agreement with the values predicted for β1,4-linkages (Satyanarayana & Rao, 1971; Imberty *et al.*, 1991). The conformation of the pentasaccharide **II** around the β1,2 linkage differs slightly from that in **I** and shows many more fluctuations (Figures 2a and 3a). The average values for $\phi 6,\psi 6$ are 53°, 2°, and these values have been shown to correspond to one of the local minima for the corresponding disaccharide moiety (Satyanarayana & Rao, 1971; Imberty *et al.*, 1991). Unlike $\phi 6$ in pentasaccharide **I**, $\phi 6$ in **II** changes frequently from about 0° to about 135°. Similarly, $\psi 6$ also shows large transitions—from −60° to 60° (Figure 3a). Either of the two weak intramolecular hydrogen bonds—between Man4–O3 and GlcNAc6–O5 or between Man4–O6 and GlcNAc6–O7—will be formed depending on the value of $\phi 6,\psi 6$. The plot showing the variation of the distance between the two terminal Gal residues with time (Figure 3d) indicates that generally they stay at a distance of approximately 15Å from one another, corresponding to an extended conformation

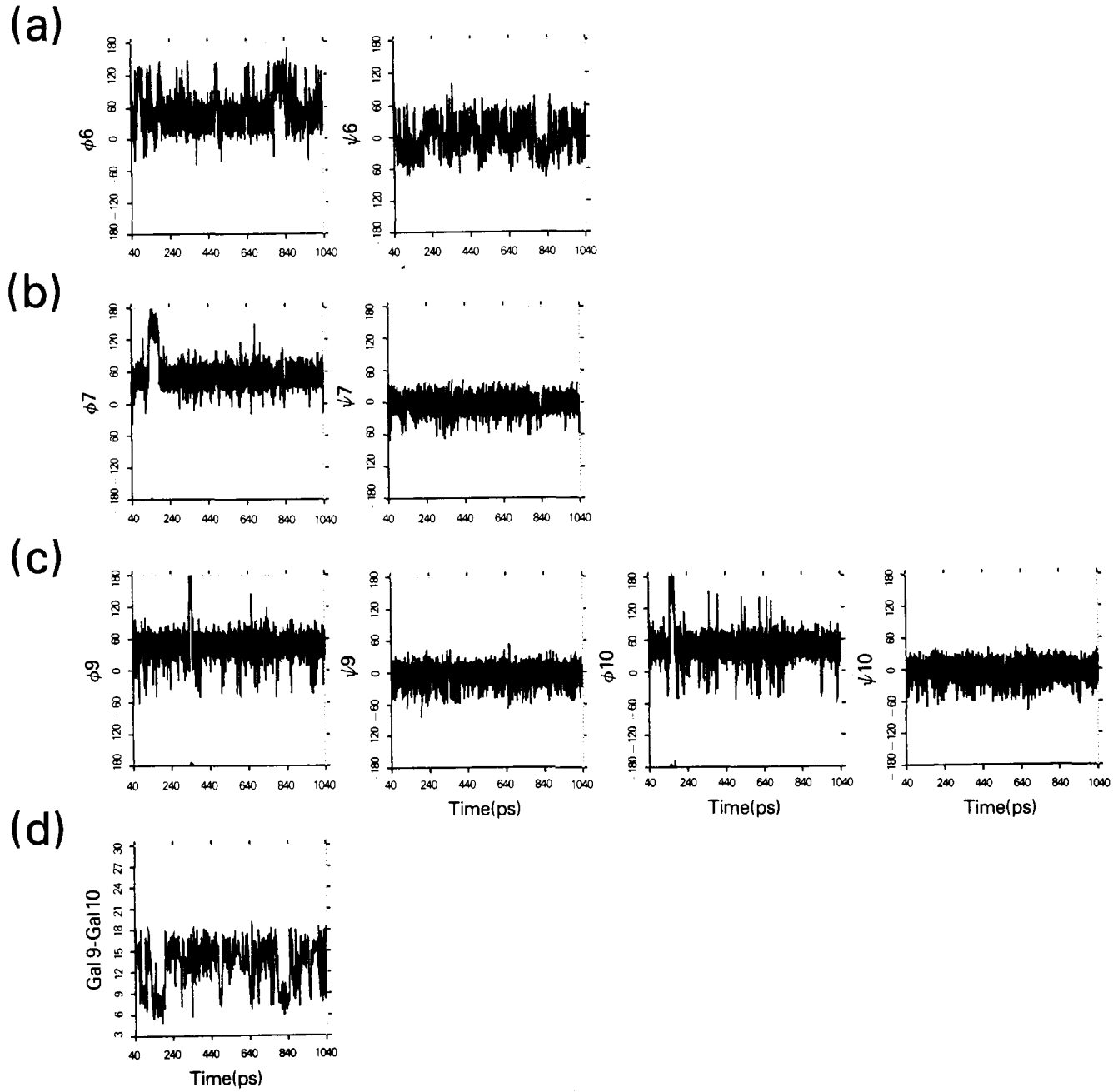

FIGURE 3: Time versus torsion angle plots extracted from the dynamic trajectory of pentasaccharide II: (a) $\phi 6,\psi 6$ for GlcNAc6-β1,2-Man4; (b) $\phi 7,\psi 7$ for GlcNAc7-β1,4-Man4; (c) $\phi 9,\psi 9$ for Gal9-β1,4-GlcNAc6 and $\phi 10,\psi 10$ for Gal10-β1,4-GlcNAc7; (d) variation in the distance between Gal9 and Gal10.

for this molecule, but occasionally the Gal residues may be as close as 6Å.

Simulation of the Triantennary Complex Oligosaccharide III. Oligosaccharide III consists of the trimannosidic core [Man4-α1,3-(Man5-α1,6)-Man3] common to all the N-linked glycans. MD simulations of oligosaccharide III were also started with three different conformers around the 1,6-linkage; i.e., $\chi 5$ = 60°, 180°, and −60° as in pentasaccharide I. Interestingly, in all three simulations, $\chi 5$ attained a final value of 60° during the equilibration period itself.

Man4-α1,3-Man3. In all three simulations, $\phi 4,\psi 4$ fluctuate about the average values 18°, −4°. From NMR studies and force-field calculations, Mazurier *et al.* (1991) and Homans (1990) favored a value of −60°, −30° for the disaccharide Man-α1,3-Man. On the other hand, Biswas *et al.* (1987) from their studies on a biantennary complex oligosaccharide favored −46°, 20° and 28°, 28° for this fragment. In fact, the average values obtained in the present simulations fall between these two sets of values. Although, in the present simulations, initial $\phi 4,\psi 4$ were taken as −50°, −25°, the average $\phi 4,\psi 4$ was found to be 18°, −4°, which corresponds to a slightly higher energy minimum for an isolated Man-α1,3-Man disaccharide.

Man5-α1,6-Man3. The average values of $\phi 5,\psi 5$ were found to be −41°, 108°. As already mentioned, irrespective of whether initial $\chi 5$ is 60° or 180° or −60°, $\chi 5$ always changes to 60° during the equilibration period. It should be noted here that the conformation with $\chi 5$ = 60° corresponds to a slightly higher energy minimum in a disaccharide fragment due to the close proximity of O4 and O6 atoms of Man3. It is possible that a hydrogen bond between O6 and the hydroxyl hydrogen at O4 offsets the repulsion between O4 and O6 atoms in this conformation.

GlcNAc6-β1,2-Man4 and GlcNAc8-β1,2-Man5. The angles $\phi 6,\psi 6$ and $\phi 8,\psi 8$ defining the conformation around the β1,2-linkage between GlcNAc and Man (Figure 1b) turned

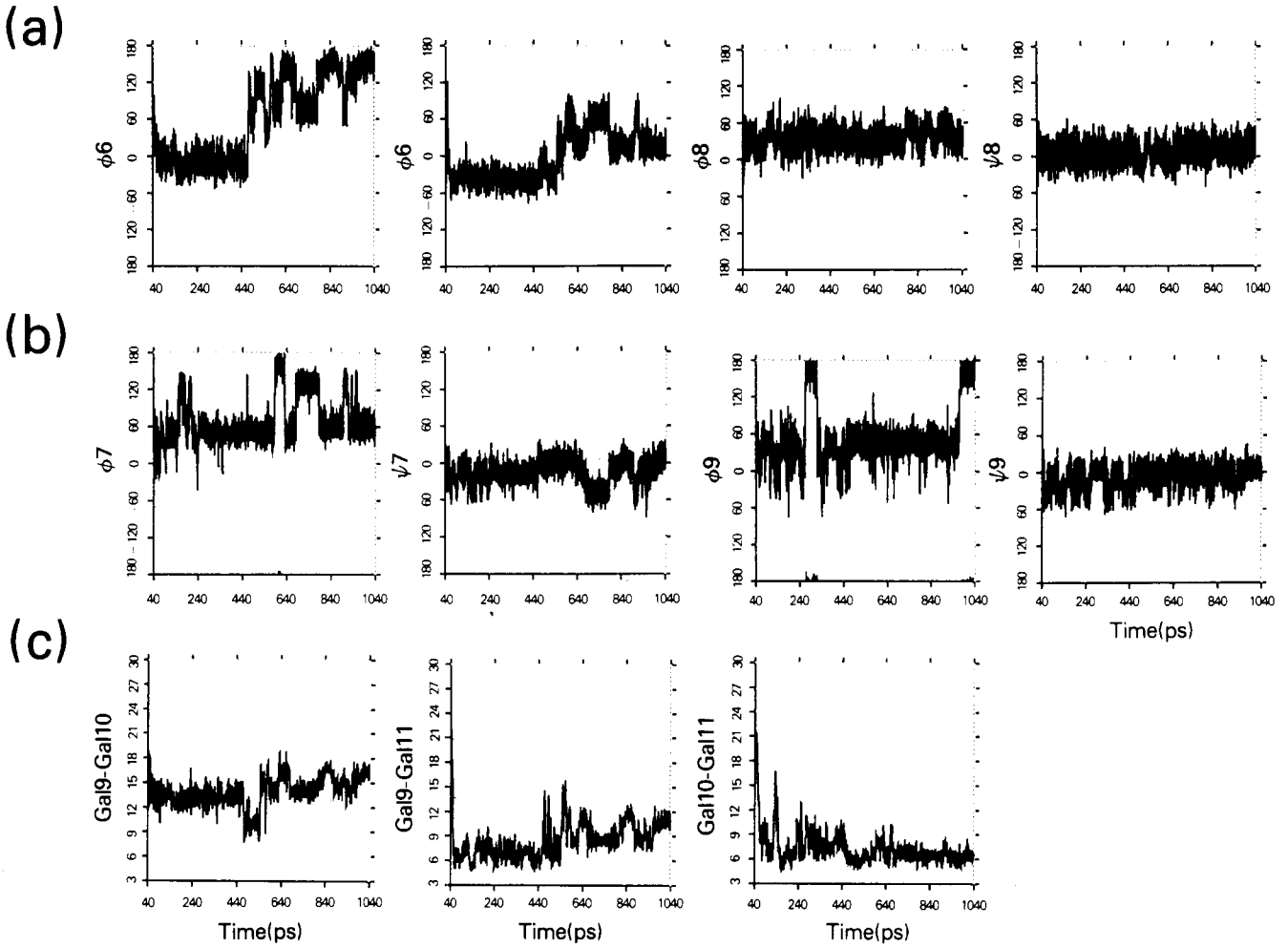

FIGURE 4: Time versus torsion angle plots for the triantennary oligosaccharide **III**: (a) $\phi 6,\psi 6$ for GlcNAc6-β1,2-Man4 and $\phi 8,\psi 8$ for GlcNAc8-β1,2-Man5 (the conformational transition seen in $\phi 6$ occurs at about 470 ps); (b) $\phi 7,\psi 7$ for GlcNAc7-β1,4-Man4 and $\phi 9,\psi 9$ for Gal9-β1,4-GlcNAc6; (c) variation in the distance between Gal9, Gal10, and Gal11. Variation of $\phi 4,\psi 4$ (mean 18°, –4°), $\phi 5,\psi 5,\chi 5$ (mean –41°, 108°, 55°), $\phi 10,\psi 10$ (mean 46°, –6°), and $\phi 11,\psi 11$ (mean 42°, –6°) are not shown since these angles show uniform fluctuations from the mean values throughout the 1000-ps simulation period.

out to be one of the interesting cases of this simulation study. In all three simulations $\phi 8,\psi 8$ have an average value of 35°, 6° and do not show any large fluctuations (Figure 4a). But this is not so for $\phi 6,\psi 6$. These angles assume two sets of conformations: one with an average value of –6°, –35° and the other 117°, 24°. The change in $\phi 6$ from –6° to 117° leads to the "flipping" of the *N*-acetyllactosamine group and thus exposes a different "face" of the saccharide to the receptor protein. Both the conformers have been predicted to correspond to low-energy conformers by previous force-field and NMR studies (Satyanarayana & Rao, 1971; Biswas *et al.*, 1987; Mazurier *et al.*, 1991; Imberty *et al.*, 1991).

β1,4-Linkages. The average values for $\phi 7,\psi 7$ which define the conformation around GlcNAc7-β1,4-Man4 obtained in these simulations (71°, –14°) are close to that observed for the minimum energy conformation for a β1,4-linked disaccharide (Satyanarayana & Rao, 1971; Imberty *et al.*, 1991). $\phi 7$ shows many more variations than $\psi 7$ (Figure 4b). Occasionally $\phi 7$ changes from 60° to 140°, leading to a change in the orientation of the *N*-acetyllactosamine group. The angles $\phi 9,\psi 9$, $\phi 10,\psi 10$, and $\phi 11,\psi 11$ around the β1,4-linkage between Gal and GlcNAc in all three antenna have average values in the same range (50°, –8° for $\phi 9,\psi 9$; 46°, –6° for $\phi 10,\psi 10$; and 42°, –6° for $\phi 11,\psi 11$). Although these angles fluctuate around the average values throughout the simulation period, the deviation from the mean is much more for $\phi 9,\psi 9$. Occasionally, $\phi 9$ jumps to 180° but returns to 60° (Figure 4b), suggesting that this Gal residue can also favor a flipped orientation.

Variation of the Distance between the Three Terminal Galactose Residues. Figure 4c shows the variation of the distance between Gal9, Gal10, and Gal11. It can be seen that Gal9 and Gal10 on the 1,2- and 1,4-branches are always separated by approximately 15Å and these two Gal residues are separated by same distance in pentasaccharide **II** also. Gal11 on the 1,6-arm comes in between the 1,2- and the 1,4-branches since $\chi 5$ takes a value around 60°.

Simulations of the Triantennary Complex Oligosaccharide **IV**. Oligosaccharide **IV** differs from **III** in having a chitobiose linked through a β1,4-linkage to Man3 of the trimannosidic core. Overall, the presence of the chitobiose core seems to affect mainly the conformation of the 1,6-arm, and the effect on the 1,3-arm seems to be less pronounced.

Man5-α1,6-Man3. The variation of the three angles, $\phi 5$, $\psi 5$, and $\chi 5$, which define the conformation around the Man5-α1,6-Man3 fragment is shown in Figure 5 for the MD simulations started with all the three initial values of $\chi 5$ (60°, 180°, and –60°; simulations 1, 2, and 3, respectively). Unlike oligosaccharide **III**, there seems to be a difference in the conformation of oligosaccharide **IV**, depending on the initial $\chi 5$ value. In the simulation which was initiated with $\chi 5$ = 60° (simulation 1), after about 920 ps, $\chi 5$ jumps to 150° and $\psi 5$ changes to 60° (Figure 5a). However, when the MD simulations were initiated with $\chi 5$ = 180° (simulation 2),

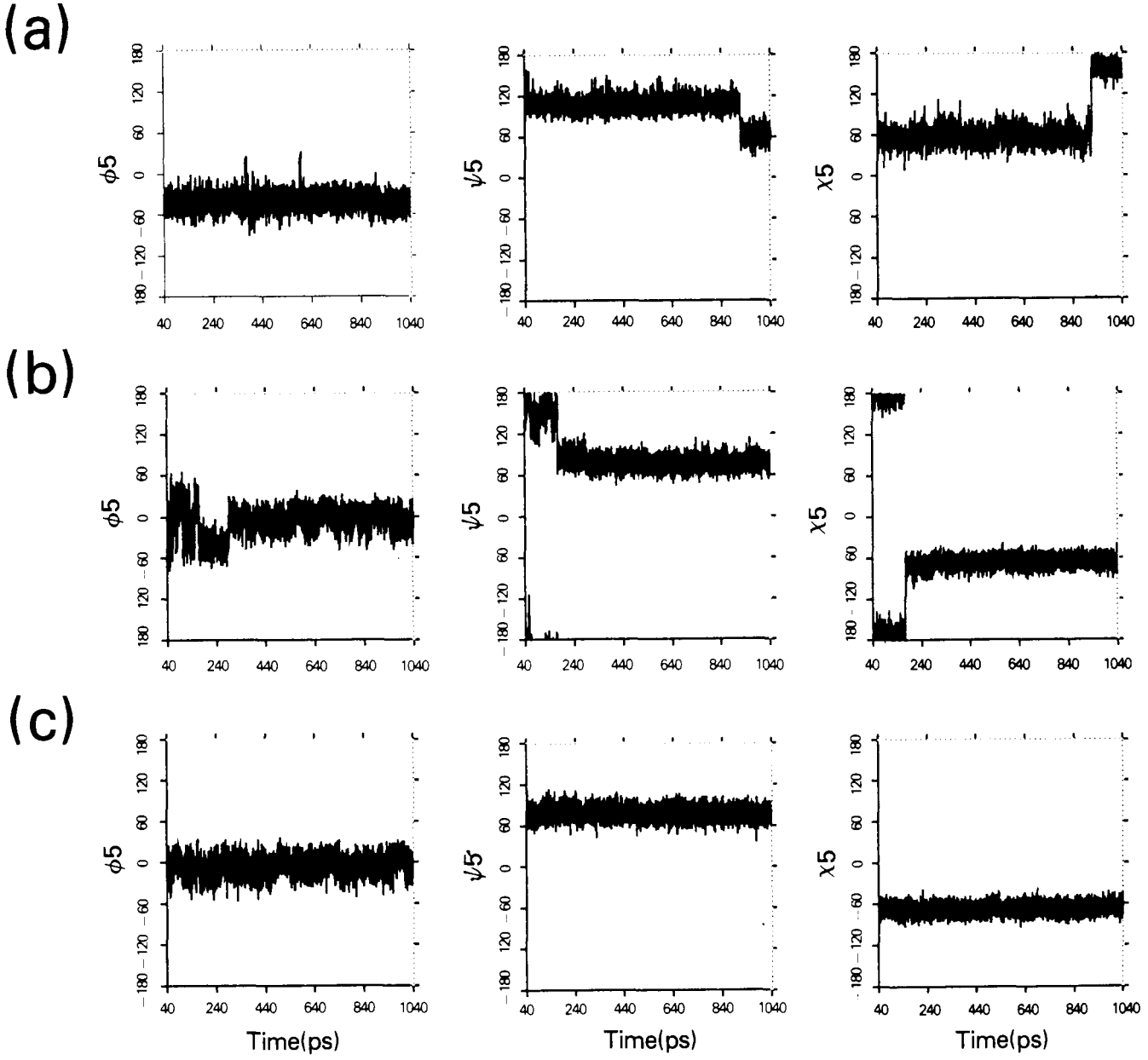

FIGURE 5: Comparison of the variation of the three torsion angles, $\phi 5$, $\psi 5$, and $\chi 5$, defining the conformation around Man5-α1,6-Man3 for different initial values of $\chi 5$ in the triantennary oligosaccharide **IV**: (a) initial $\chi 5 = 60°$; (b) initial $\chi 5 = 180°$; (c) initial $\chi 5 = -60°$.

after about 200 ps, $\chi 5$ jumps to $-60°$ with a concomitant change in $\psi 5$ from around 180° to around 70° (Figure 5b). When the MD simulation was started with $-60°$ (simulation 3), $\chi 5$ remains at $-60°$ (Figure 5c). In all the three simulations, $\phi 5$, $\psi 5$, and $\chi 5$ fluctuate around the corresponding average values with a mean deviation of ±15°.

Core β1,4-Linkages. $\phi 2,\psi 2$ and $\phi 3,\psi 3$ which determine the conformation around the β1,4-linkages in the core were set initially at 60°, 0° in all three simulations. None of these four angles show any significant deviations from the initial values throughout the simulation period. A similar observation was made from the molecular dynamics simulations of Man-α1,3-Man-β1,4-GlcNAc both with and without explicit solvent molecules (Homans, 1990). Hence the variation of $\phi 2,\psi 2$ and $\phi 3,\psi 3$ is shown only for simulation 2 (Figure 6a,b). Hydrogen bonds from GlcNAc1–O3 to GlcNAc2–O5 and from GlcNAc2–O3 to Man3–O5 were found to be maintained in all three simulations. It was observed that the exocyclic torsion angle χ which determines the conformation of the CH_2OH group at C5 accesses all three staggered conformations and hydrogen bonds from GlcNAc1–O6 to GlcNAc2–O7 and from GlcNAc1–O3 to GlcNAc2–O6 are possible when χ(GlcNAc1) = *gauche*$^+$ and χ(GlcNAc2) = *gauche*$^-$ or *trans*, respectively.

Man4-α1,3-Man3. In simulations 1 and 3, $\phi 4,\psi 4$ fluctuate around 30°, 30° throughout the 1000-ps period. However, in simulation 2, $\phi 4$ shows a large variation from $-80°$ to 120° (Figure 6c). It thus samples almost all the conformational space available for the Man-α1,3-Man disaccharide fragment (Satyanarayana & Rao, 1972; Homans, 1990). A hydrogen bond between Man4–O2 and Man3–O5 is also possible whenever $\phi 4$ is around $-30°$ and $\psi 4$ is around 30°. The values of $\phi 4$ and $\psi 4$ reported here are in agreement with those reported by Biswas *et al.* (1987) and Imberty *et al.* (1990). Interestingly, it was observed that, in the simulation of all the oligosaccharides, there is a strong correlation between the angles $\phi 4$ and $\chi 5$. Whenever $\chi 5$ is around 180°, $\phi 4$ tends to be around $-45°$ (Figures 5 and 6c). When $\chi 5$ changes to either $-60°$ or 60°, $\phi 4$ changes to values around 20°. Thus conformation of Man5 appears to be fine tuned by the conformation of Man4 and vice versa.

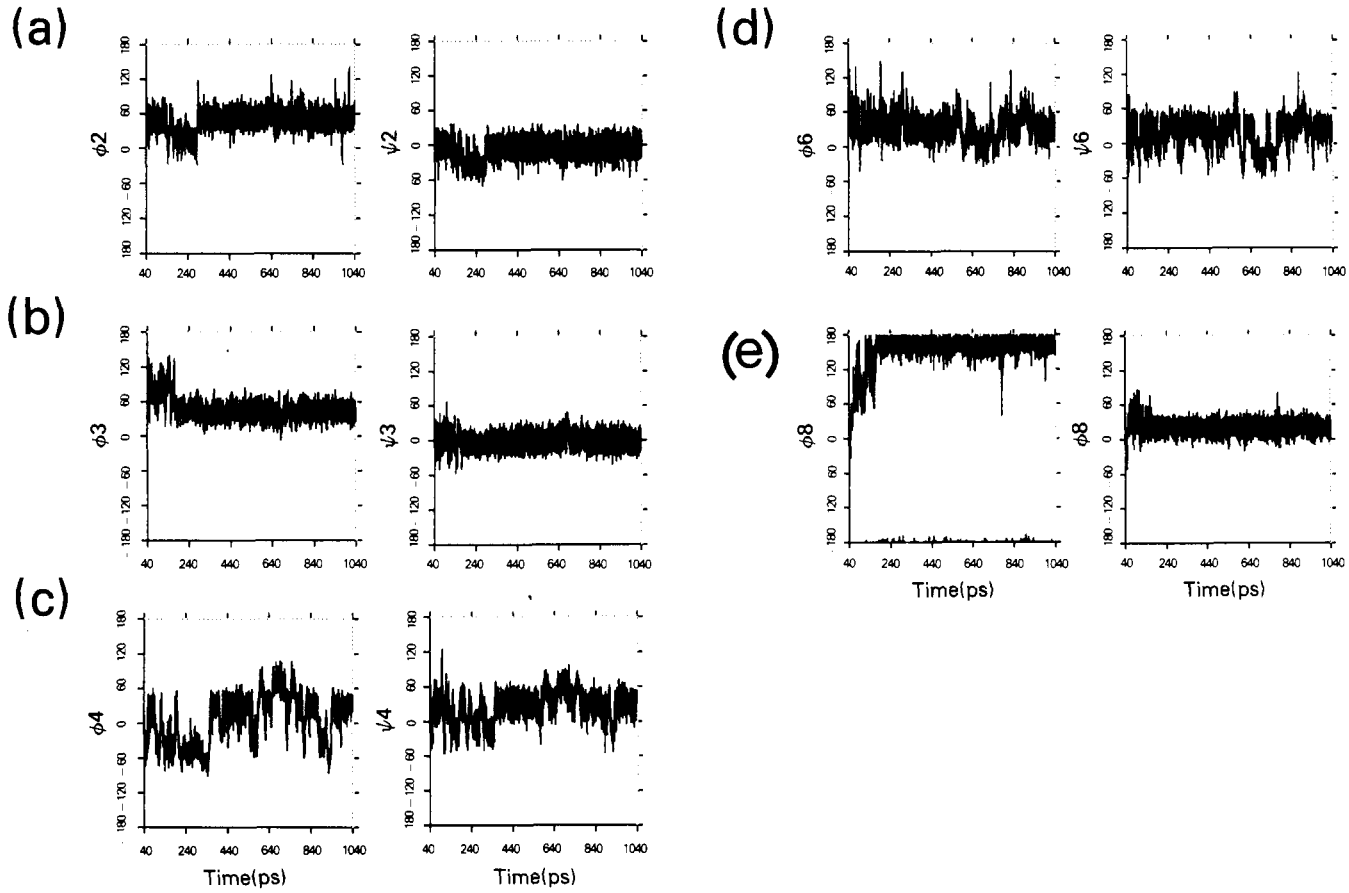

FIGURE 6: Time versus torsion angle plots for (a) $\phi 2,\psi 2$ around GlcNAc2-β1,4-GlcNAc1, (b) $\phi 3,\psi 3$ around Man3-β1,4-GlcNAc2, (c) $\phi 4,\psi 4$ around Man4-α1,3-Man3, (d) $\phi 6,\psi 6$ around GlcNAc6-β1,2-Man4, and (e) $\phi 8,\psi 8$ around GlcNAc8-β1,2-Man5 obtained from the dynamics trajectory of the triantennary oligosaccharide **IV** (initial $\chi 5 = 180°$). Panels d and e compare the behavior of the torsion angles around the β1,2-linkage between GlcNAc and Man in the 1,3- and 1,6-arms. Time versus torsion angle plots for $\phi 7,\psi 7$ (GlcNAc7-β1,4-Man4), $\phi 9,\psi 9$ (Gal9-β1,4-GlcNAc6), $\phi 10,\psi 10$ (Gal10-β1,4-GlcNAc7) and $\phi 11,\psi 11$ (Gal11-β1,4-GlcNAc8) are not shown since these angles show uniform fluctuations from the mean values throughout the 1000-ps simulation period.

GlcNAc6-β1,2-Man4 and GlcNAc8-β1,2-Man5. As mentioned earlier, the angles $\phi 6,\psi 6$ and $\phi 8,\psi 8$ defining the conformation around the β1,2-linkage between GlcNAc and Man turn out to be the most interesting case of this simulation study. $\phi 6,\psi 6$ fluctuate more than $\phi 8,\psi 8$ in all three simulations (Figure 6d,e). The conformational angles $\phi 8,\psi 8$ were found to be strongly linked to $\chi 5$. Whenever $\chi 5$ takes a value around $-60°$ (Figure 5b,c), $\phi 8$ changes from around 60° to a value near 180°; i.e., for this conformation of $\chi 5$, the *N*-acetyllactosamine residue favors a flipped conformation. In fact, in the crystal structure of the human Fc fragment and its complex with fragment B of protein A where $\phi 5$ was found to be close to 180°, $\chi 5$ is around $-60°$ (Deisenhofer, 1981). Such a conformation for the β1,2-linked GlcNAc was not predicted by the earlier NOE experiments (Carver & Brisson, 1984). In all three simulations, however, $\phi 5,\psi 5,\chi 5$ and $\phi 8,\psi 8$ which determine the conformation of the 1,6-arm show less fluctuations than $\phi 4,\psi 4$ and $\phi 6,\psi 6$—angles which define the conformation of the 1,3-arm. Hydrogen bonds from Man4–O3 to GlcNAc6–O5 and from Man5–O3 to GlcNAc8–O5 are possible when $\phi 6,\psi 6$ and $\phi 8,\psi 8$ are in the 60°, 0° region. The latter hydrogen bond is lost when $\phi 8$ takes up a value near 180°.

β1,4-Linkages. Angles $\phi 7,\psi 7$ which define the conformation between GlcNAc7 and Man4 do not show any large variation in any of the simulations. The mean $\phi 7,\psi 7$ is 60°, 0°. The Man4–O3 to GlcNAc7–O5 hydrogen bond is maintained throughout the simulation period. It should be noted here that Man4–O3 can form a hydrogen bond with GlcNAc6–O5 also (connected through a β1,2-linkage). As in the case of GlcNAc2-β1,4-GlcNAc1, hydrogen bonds between Man4–O6 and GlcNAc7–O7 (when χ of Man4 is *gauche*$^+$) and from Man4–O3 to GlcNAc7–O6 (when χ of GlcNAc7 is *gauche*$^-$ or *trans*) atoms are also possible. The angles $\phi 9,\psi 9$, $\phi 10,\psi 10$, and $\phi 11,\psi 11$ around the β1,4-linkage between the terminal Gal and GlcNAc in all three antenna fluctuate around 60°, 0°. However, the mean deviation is much more than those seen for other angles, probably because they define the conformation of a terminal residue. Occasionally, they jump to a 180°, 0° conformation but come back to a 60°, 0° conformation before too long. In the three terminal *N*-acetyllactosamine groups, Gal9-GlcNAc6, Gal10-GlcNAc7, and Gal11-GlcNAc8, hydrogen bonds from GlcNAc–O3 to Gal–O5 and between Gal–O2 and GlcNAc–O6 (when χ of GlcNAc is around 60°) are possible except when ϕ jumps from around 60° to around 180°. Interestingly, Imberty *et al.* (1991) report that the GlcNAc–O3 to Gal–O5 hydrogen bond is possible even when ϕ,ψ are around 180°, 0° and, in this conformation, such a hydrogen bond appears to be stereochemically less likely.

Distance between the Terminal Galactose Residues. A plot of the distance between the terminal Gal residues from GlcNAc1 of the core and between themselves is shown in Figure 7. It is very interesting to see that Gal9 and Gal10, which are on the 1,3-arm, show much more variation than Gal11, which is on the 1,6-arm (Figure 7a). This is interesting since all the earlier studies have predicted that whatever little "flexibility" the oligosaccharides show lies in the 1,6-arm and not in the 1,3-arm (Carver & Brisson, 1984). It can also be seen from Figure 7a that even though Gal9 and Gal10 show

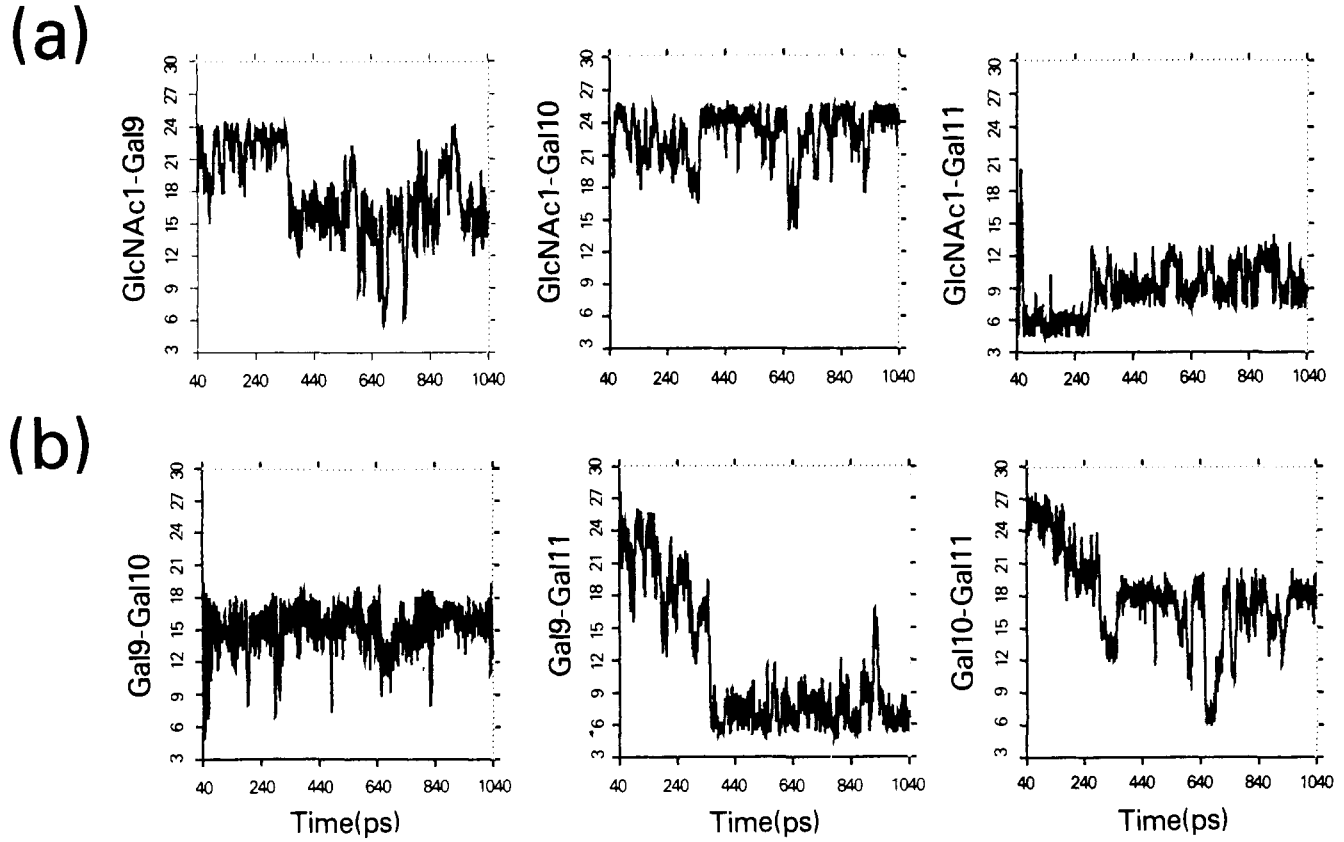

FIGURE 7: Variation of the distance between the core GlcNAc1 and the three terminal Gal residues, Gal9, Gal10, and Gal11 (a), and between the terminal Gal residues themselves (b) during the simulation of oligosaccharide IV (initial $\chi 5 = 180°$).

a considerable degree of flexibility, the distance between them remains very nearly constant (Figure 7b). The separation between these Gal residues seen in this oligosaccharide IV (15Å) is very close to what is observed in the simulations of oligosaccharide III (Figure 4) and in pentasaccharide II (Figure 3). This shows that the distance between these two Gal residues is the same irrespective of whether they are in pentasaccharide II or oligosaccharides III and IV. The distance of Gal11 from Gal9 and Gal10 decreases after about 200 ps, and the distance between Gal11 and GlcNAc1 increases simultaneously (Figure 7b). This indicates that, during the course of simulation, the 1,6-arm moves away from the core GlcNAc1 and toward the 1,3-arm. Of all the three Gal residues, Gal11 of the 1,6-arm is the closest to the core GlcNAc1.

Intramolecular Hydrogen Bonds between Noncontiguous Residues. A systematic analysis of the dynamics trajectories was carried out to search for possible intramolecular hydrogen bonds between noncontiguous residues also. It was found that, depending on $\chi 5$, the 1,6-arm residues form hydrogen bonds either with one of the core chitobiose residues ($\chi 5$ around $-60°$) or with the 1,4-branch residues ($\chi 5$ around $60°$). No hydrogen bonds were seen between either the 1,2-branch and the 1,4-branch or the core chitobiose and the 1,3-arm in any of the conformations of oligosaccharide IV. When $\chi 5$ is around $60°$, 1,4-branch and 1,6-arm residues are close enough to have possible hydrogen-bonding interactions. Hydrogen bonds from Man4–O3 to either GlcNAc8–HN or GlcNAc8–O4 and from GlcNAc8–O3 to GlcNAc7–O7 are possible in this conformation. In addition, when χ of Gal11 is in a *gauche*$^-$ conformation, Gal11–O6 can form hydrogen bonds with GlcNAc7–O7. When $\chi 5$ is around $-60°$, hydrogen bonds between GlcNAc1–O3 and GlcNAc8–O7, GlcNAc2–O7 and Man5–O3, GlcNAc2–O7 and Man5–O4, and Man3–O4 and GlcNAc8–O6 (χ–GlcNAc8 around $180°$) are possible, and these hydrogen bonds are fairly well maintained during the simulation. In addition to these, hydrogen bonds between GlcNAc1–O7 and Gal11–O6 (χ–Gal11 around $180°$), GlcNAc2–O6 (χ–GlcNAc2 around $\pm$*gauche*) and Gal11–O6 (χ–Gal11 around $180°$), and GlcNAc6–HN and Gal11–O2 are also possible but are less frequent. Thus, the 1,6-arm shows extensive hydrogen-bonding interactions with the core chitobiose in this conformation ($\chi 5$ around $-60°$) of oligosaccharide IV. It should, however, be noted that some of the hydrogen bonds mentioned here may be weakened or broken either when it interacts with the asialoglycoprotein or any other receptor or when the oligosaccharide is solvated due to competition by solvent molecules to form hydrogen bonds. In fact, a comparison of the dynamics simulations of cellobiose in water and in vacuo showed that intramolecular hydrogen bonds observed in the in vacuo simulations are weakened in the presence of explicit water molecules (Hardy & Sarko, 1993b). This cellobiose simulation also showed that the solvent molecules form hydrogen bonds only with the pendant hydroxyls and not with the ring or the glycosidic oxygen. The conformation of the hydroxymethyl group at C5 has also been shown to be influenced by solvent molecules (Kroon-Batenburg & Kroon, 1990).

DISCUSSION

Most of the earlier simulation studies of oligosaccharides have been carried out for periods ranging from 10 to 500 ps (Dauchez *et al.*, 1992; Edge *et al.*, 1990; Hardy & Sarko, 1993a; Homans, 1990; Homans *et al.*, 1987; Mukhopadhyay & Bush, 1991; Prabhakaran, 1991). It is not known whether simulations of this length sample sufficiently all the available conformational space. It has also been felt that longer simulations are necessary for proper statistical sampling of torsion angle space while interpreting NOE data (Carver *et al.*, 1990). Hence, in the present study, the four oligosac-

charides studied were simulated for 1000 ps. It can be seen from Figures 2b,c, 3a,b, 5, and 6 that significant conformational transitions occur even after 500 ps in many torsion angles, indicating that longer simulation periods are indeed required for an exhaustive search of the conformational energy surface. The results presented here also show that the nature of the dynamics trajectories obtained is independent of the initial value of χ (in 1,6-linkage) for smaller oligosaccharides. But the trajectories were different for different initial values of χ for oligosacchride **IV**. This suggests that even simulations for 1000 ps with a single initial conformation are not sufficient to sample all the conformations available for larger, branched oligosaccharides and hence it is essential that simulations should be carried out by starting from all three staggered orientations for χ in 1,6-linkages.

Flexibility of the Oligosaccharide. Classically, oligosaccharides have been thought to be relatively "rigid" molecules, meaning they show little variability in their conformations (Carver & Brisson, 1984; Homans *et al.*, 1986, 1987). Whatever little flexibility exists was associated with the 1,6-linkage since there are three bonds around which rotations can be made in a 1,6-linkage. But results from the present study show that oligosaccharides are "flexible" molecules showing significant conformational variability. This is clearly reflected in the plots of inter-galactose distances versus time (Figures 3, 4, and 7). Such a conformational flexibility has also been observed from molecular dynamics simulations of a monofucosylated, sialylated biantennary *N*-acetyllactosamine type of oligosaccharide (Dauchez *et al.*, 1992). Since oligosaccharides simulated in the present study are triantennary and lack fucose and sialic acid, a direct comparison between the results of the two simulations has not been done. From NMR studies on di- and trisaccharides (Cumming *et al.*, 1987), it has been hypothesized that the hydrogen bond between Man4–O3 and GlcNAc7–O5 introduces a high degree of segmental constraint and hence decreases the flexibility of *N*-acetyllactosamine-type complex oligosaccharides. However, it can be seen from these figures that the variation in distance with time is more for the Gal residues on the 1,3-arm compared to the Gal residue on the 1,6-arm, indicating that in this oligosaccharide the 1,3-arm is much more flexible than the 1,6-arm. This flexibility for the 1,3-arm Gal residues mainly arises from the α1,3-linkage between Man3 and Man4 and the β1,2-linkage between Man4 and GlcNAc6.

Importance of 180°, 0° Conformation for β1,4- and β1,2-Linkages. Although the torsion angles ϕ,ψ between GlcNAc-β1,2-Man fluctuate around some of the minimum energy conformations most of the time (Figures 3, 4, and 6), ϕ shows transitions to 180° also. This conformation also corresponds to a local minimum from force field calculations on disaccharide fragments. The present dynamics study shows that the energy barrier between these conformations can be easily crossed. This conformational transition to ϕ = 180° leads to "flipping" of the *N*-acetyllactosamine group, and this may be important for certain oligosaccharides for recognition by the respective receptors. In the crystal structure of the human Fc fragment and its complex with fragment B of protein A from *Staphylococcus aureus*, such a conformation has indeed been observed for the β1,2-linkage (Deisenhofer, 1981). This type of conformational change has been observed in the present study for β1,4-linkages also. But such a possibility was not considered while proposing models for complex oligosaccharides by the earlier workers. The terminal Gal residues which are recognized by the ASGP-R are connected to GlcNAc by a β1,4-linkage. Hence, it is possible that some galactose residues may "flip" when they bind to the receptor. Molecular dynamics simulations were also carried out for the oligosaccharide β1,3-**IV**, oligosaccharide **IV** with a β1,3-linkage between GlcNAc7 and Gal10 instead of β1,4-linkage, and these simulations showed that the transition to the 180°, 0° conformation was possible for β1,3-linkages also (data not shown).

Effect of the Chitobiose Core on the Conformation of the Triantennary Oligosaccharide. Oligosaccharide **IV** differs from **III** in having a chitobiose attached to the Man3 of the trimannosidic core in a β1,4-linkage. GlcNAc1, GlcNAc2, Man3, Man4, and Man5 constitute the classic "core" seen in all the N-linked glycoproteins. Molecular dynamics simulations of both oligosaccharides were done with nearly the same starting conformations and with all three staggered conformations for χ5. The behavior of all the torsion angles in the 1,3-arm was found to be very similar in the two molecules, implying that the presence or absence of the chitobiose does not drastically affect the conformational preferences of the 1,3-arm. However, the conformation of the 1,6-arm showed a remarkable difference in the two triantennary oligosaccharides. In the absence of the chitobiose core, the 1,6-arm was found to be closer to the 1,2- and 1,4-branches of the 1,3-arm. However, this is not the case when the chitobiose core is present on Man3. Generally, in oligosaccharide **IV**, the 1,6-arm tends to come closer to the chitobiose core (Figure 8). However, in a glycoprotein, the conformation of this 1,6-arm may be influenced by the amino acid residues around the glycosylation site.

Binding Affinities of Pentasaccharides **I** *and* **II** *to ASGP-R.* The results obtained from the present molecular dynamics simulation study, in addition to providing information about the conformational preferences of these oligosaccharides, are also useful in understanding the differences in the binding affinities of these molecules to ASGP-R. Pentasaccharide **I** differs from **II** in having a β1,6-linkage instead of β1,4-linkage between Man4 and GlcNAc7. However, pentasaccharide **II** shows a nearly 15-fold higher affinity to ASGP-R than pentasaccharide **I**. According to the golden triangle hypothesis (Lee *et al.*, 1984), the affinity of ligands to ASGP-R depends on the number of Gal residues present in the ligand and the distance separating them. Both pentasaccharides **I** and **II** have two terminal Gal residues. Molecular dynamics simulations of these oligosaccharides have shown that the distance between the terminal Gal residues in pentasaccharide **II** is about 15Å during most of the simulation period (Figure 3d) and pentasaccharide **I** can access conformations in which the Gal residues are separated by 15Å (Figure 2d). It thus seems that the number of terminal Gal residues and the distance between them, the factors considered in the earlier models, alone are not sufficient to explain the experimental data. Figure 9 shows the common trisaccharide fragment (Man4-β1,2-GlcNAc6-β1,4-Gal9) of pentasaccharide **I** superposed over that of **II**. From this figure it can be seen that although Gal9 is in the same orientation in both the oligosaccharides, Gal10 and Gal10′ are placed differently in the two pentasaccharides. Hence, while binding to the two Gal binding sites of the ASGP-R, if Gal9 occupies one of the binding site, then Gal10′ in pentasaccharide **I** cannot occupy the second binding site which is accessible to Gal10. Hence, ASGP-R can accommodate either Gal9 or Gal10′ of pentasaccharide **I** in the galactose binding site and not both of them simultaneously leading to weak binding compared to **II**. Thus the present molecular dynamics studies suggest that the proper distance between the Gal residues is a necessary but not sufficient condition. Recognition of the oligosaccharide by the receptor requires, in addition to the proper separation, correct orientation of the

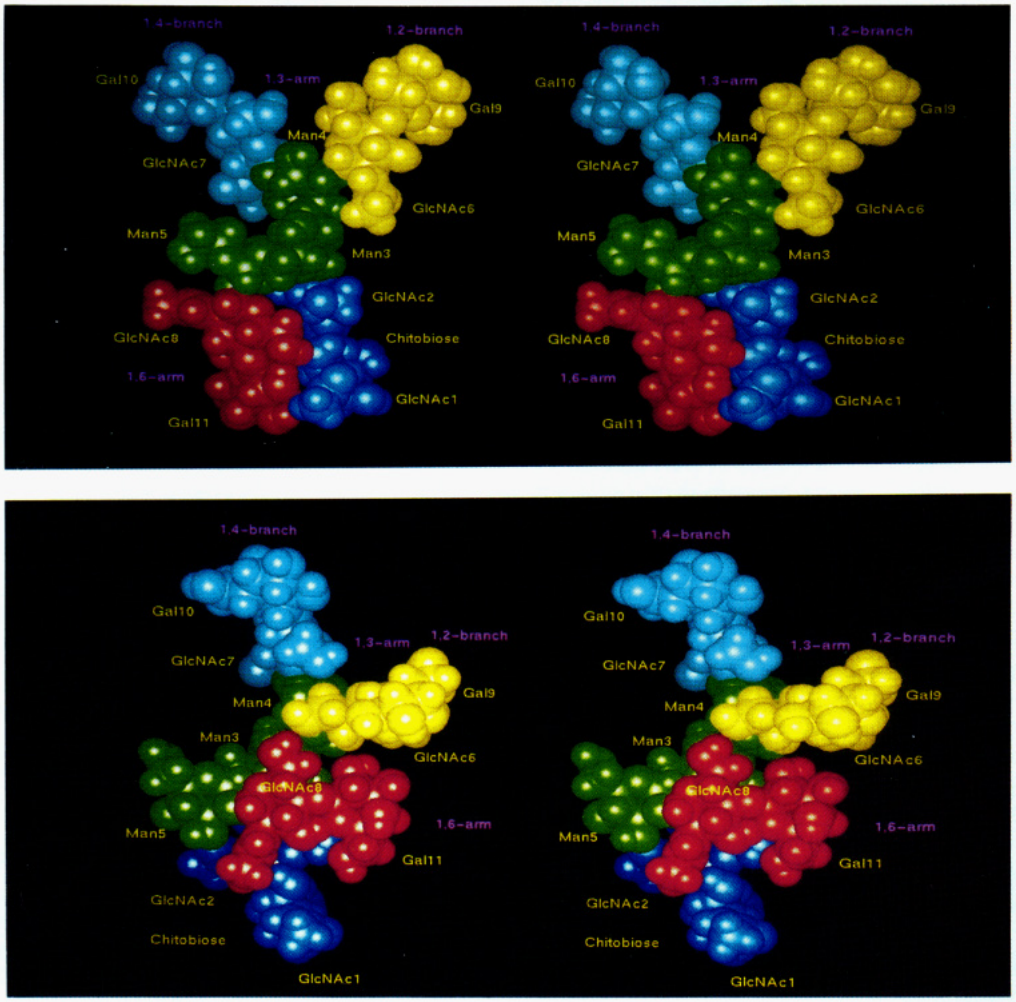

FIGURE 8: Two conformations of the 1,6-arm accessed by triantennary oligosaccharide **IV** during MD simulations. Stereo diagrams taken after 100 ps (a, top) and 500 ps (b, bottom) (initial $\chi 5 = 180°$). In panel a, $\chi 5$ is around 180° and the 1,6-arm (red) is parallel to the chitobiose core (blue); in panel b, $\chi 5$ is around –60° and the 1,6-arm is perpendicular to the chitobiose core. Color codes for other residues are as follows: trimannosidic core, green; 1,2-branch, yellow; 1,4-branch, cyan.

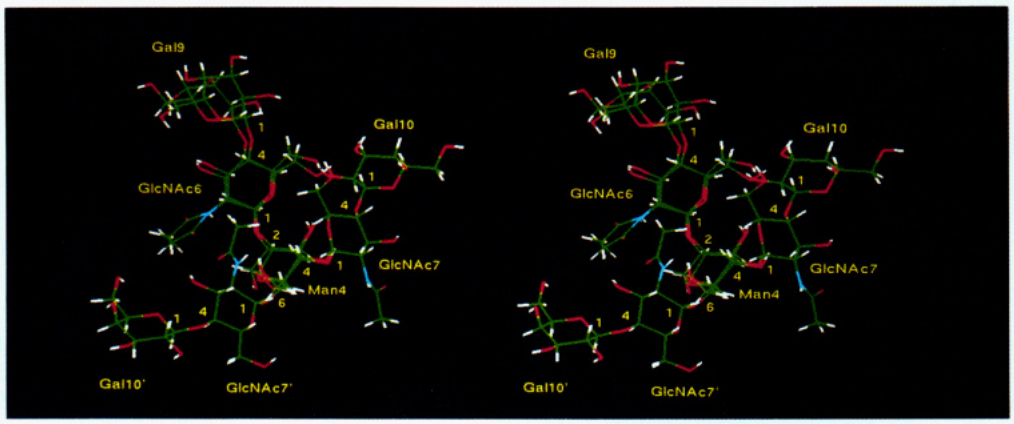

FIGURE 9: Stereo diagram showing pentasaccharide **I** (taken after 79.6 ps) superposed over pentasaccharide **II** (taken after 370.3 ps). GlcNAc6 and Gal9, whose orientation is similar in both **I** and **II**, are taken as reference points for superposition. The orientation of GlcNAc7′ and Gal10′ (pentasaccharide **I**) is different from that of GlcNAc7 and Gal10 (**II**). The distance between the two Gal residues is 17.3Å in **I** and 17.7Å in **II**.

Gal residues with respect to one another.

A Modified Model for the Binding of Oligosaccharides to ASGP-R. As mentioned earlier, triantennary oligosaccharide **IV** shows the highest affinity to ASGP-R. In this oligosaccharide, the 1,6-arm displays two discrete conformations and was found to be close to the chitobiose core during most of the simulation period, an observation which has been corroborated by NMR and fluorescence studies (Wu *et al.*, 1991). The 1,2- and 1,4-branches on the 1,3-arm will be pointing away from the core in all the conformations, and the distance between the terminal galactose residues on the 1,2- and 1,4-branches is very nearly the same in pentasaccharide **II** and oligosaccharides **III** and **IV**. Oligosaccharides containing the 1,2- and 1,4-branches show higher affinity to ASGP-R than those where one of these branches is missing (Lodish, 1991). On the basis of these results together with the present analysis,

it is proposed that only Gal9 of the 1,2-branch and Gal10 of the 1,4-branch are crucial for recognition by ASGP-R. Binding of Gal9 and Gal10 to the receptor sites may bring about a conformational change in the 1,6-arm leading to additional interactions between the oligosaccharide and ASGP-R contributing to the binding energy and internalization. This model explains the higher binding affinity of pentasaccharide **II** (where the 1,6-arm is missing) compared to a biantennary oligosaccharide which lacks the 1,4-branch (Lodish, 1991).

Bovine fetuin has been found to contain a triantennary oligosaccharide (β1,3-**IV**) which differs from oligosaccharide **IV** in having a β1,3-linkage instead of β1,4 between GlcNAc7 and Gal10. This oligosaccharide with β1,3-linkage binds to ASGP-R nearly hundredfold less tightly than oligosaccharide **IV**. In the preferred conformations of oligosaccharides **IV** and β1,3-**IV**, only the relative orientation of Gal9 and Gal10 are different but not the distance between them (data not shown). Interestingly, the relative orientation of Gal9 and Gal10 in oligosaccharide β1,3-**IV** will be fairly close to that in oligosaccharide **IV** if GlcNAc7-β1,3-Gal10 fragment takes up a conformation around 180°, 0°. Such an orientation for Gal10 is possible but less frequent due to higher conformational energy. This perhaps explains the lower binding affinity of β1,3-**IV** to ASGP-R compared to oligosaccharide **IV**. It has also been found that the protomers constituting ASGP-R have a similar amino acid sequence at the carboxy terminus where the Gal binding sites are located. Since only two Gal residues are recognized by the receptor and since both the protomers of ASGP-R are required for receptor activity, the possibility that the Gal binding sites are located at the interface of the two protomers cannot be ruled out.

CONCLUSIONS

Some of the conclusions that are drawn from the present study are as follows: (1) Oligosaccharides show a considerable amount of flexibility contrary to earlier beliefs. (2) The two terminal Gal residues on the 1,3-arm may primarily be recognized by ASGP-R followed by the interaction of Gal on the 1,6-arm, providing additional binding energy. (3) In addition to the proper distance between the terminal Gal residues that is necessary for recognition by ASGP-R, the relative orientation of the two Gal residues is also crucial for binding. (4) The present study also provides a theoretical basis for the observed differences in the binding characteristics of various bi- and triantennary oligosaccharides to ASGP-R.

NOTE ADDED IN PROOF

On the basis of the modified model proposed here, a triantennary oligosaccharide wherein GlcNAc7-Gal10 (1,4-branch) is linked to Man5 (1,6-arm) instead of Man4 (1,3-arm) as in oligosaccharide **IV** may bind to ASGP-R weakly compared to **IV**, which is in agreement with the experimental results (Y.C. Lee, personal communication).

ACKNOWLEDGMENT

The authors thank Drs. J. V. Maizel, G. Ashwell, Y. C. Lee, A. S. Masibay, and E. E. Boeggeman for helpful discussions. They also thank Dr. Rick Gussio for his help while using InsightII. The authors acknowledge the National Cancer Institute for allocation of computing time and staff support at the Frederick Biomedical Supercomputing Center of the Frederick Cancer Research and Development Center.

REFERENCES

Arnott, S., & Scott, W. E. (1972) *J. Chem. Soc., Perkin Trans. 2*, 324–335.

Ashwell, G., & Harfold, J. (1982) *Annu. Rev. Biochem. 51*, 532–554.

Biswas, M., Sekharudu, Y. C., & Rao, V. S. R. (1987) *Carbohydr. Res. 160*, 151–170.

Brady, J. W. (1991) *Curr. Opin. Struct. Biol. 1*, 711–715.

Brandley, B. K., Swiedler, S. J., & Robbins, P. W. (1990) *Cell 63*, 861–863.

Carver, J. P., & Brisson, J.-R. (1984) in The *Biology of Carbohydrates* (Ginsburg, V., & Robbins, P. W., Eds.) Vol. 2, pp 289–331, John Wiley & Sons, New York.

Carver, J. P., Mandel, D., Michnick, S. W., Imberty, A., & Brady, J. W. (1990) in *Computer modelling of carbohydrate molecules* (French, A. D., & Brady, J. W., Eds.) ACS Symposium Series 430, pp 266–280, American Chemical Society, Washington, DC.

Corey, R. B., & Pauling, L. (1953) *Proc. R. Soc. London, Ser. B 141*, 10–20.

Cumming, D. A., Shah, R. N., Krepinsky, J. J., Grey, A. A., & Carver, J. P. (1987) *Biochemistry 26*, 6655–6663.

Dauchez, M., Mazurier, J., Montreuil, J., Spik, G., & Vergoten, G. (1992) *Biochimie 74*, 63–74.

Deisenhofer, J. (1981) *Biochemistry 20*, 2361–2370.

Edge, C. J., Singh, U. C., Bazzo, R., Taylor, G. L., Dwek, R. A., & Rademacher, T. W. (1990) *Biochemistry 29*, 1971–1974.

French, A. D., & Brady, J. W. (1990) in *Computer modelling of carbohydrate molecules* (French, A. D., & Brady, J. W., Eds.) ACS Symposium Series 430, pp 1–19, American Chemical Society, Washington, DC.

French, A. D., Rowland, R. S., & Allinger, N. L. (1990) in *Computer modelling of carbohydrate molecules* (French, A. D., & Brady, J. W., Eds.) ACS Symposium Series 430, pp 120–140, American Chemical society, Washington, DC.

Hardy, B. J., & Sarko, A. (1993a) *J. Comput. Chem. 7*, 831–847.

Hardy, B. J., & Sarko, A. (1993b) *J. Comput. Chem. 7*, 848–857.

Homans, S. W. (1990) *Biochemistry 29*, 9110–9118.

Homans, S. W., Dwek, R. A., Boyd, J., Mahmoudian, M., Richards, W. G., & Rademacher, T. W. (1986) *Biochemistry 25*, 6342–6340.

Homans, S. W., Pastore, A., Dwek, R. A., & Rademacher, T. W. (1987) *Biochemistry 26*, 6649–6655.

Imberty, A., Gerber, S., Tran, V., & Perez, S. (1990) *Glycoconjugate J. 7*, 27–54.

Imberty, A., Delage, M.-M., Bourne, Y., Cambillau, C., & Perez, S. (1991) *Glycoconjugate J. 8*, 456–483.

Kroon-Batenburg, L. M. J., & Kroon, J. (1990) *Biopolymers 29*, 1243–1248.

Lee, R. T. (1991) in *Liver diseases* (Wu, G. Y., & Wu, C. H., Eds.) pp 65–86, Marcel Dekker, New York.

Lee, Y. C. (1989) *Ciba Found. Symp. 145*, 80–95.

Lee, Y. C., Townsend, R. R., Hardy, M. R., Loenngren, J., Arnart, J., Haraldsson, M., & Loenn, H. (1983) *J. Biol. Chem. 258*, 199–202.

Lee, Y. C., Townsend, R. R., Hardy, M. R., Loenngren, J., & Bock, K. (1984) in *Biochemical and biophysical studies of proteins and nucleic acids* (Lo, T. B., Liu, T. Y., & Li, C. H., Eds.) pp 349–360, Elsevier, New York.

Lodish, H. F. (1991) *Trends Biochem. Sci. 16*, 373–377.

Mazurier, J., Dauchez, M., Vergoten, G., Montreuil, J., & Spik, G. (1991) *Glycoconjugate J. 8*, 390–399.

Mohan, S. (1993) Ph.D. Thesis, Indian Institute of Science, Bangalore, India.

Mukhopadhyay, C., & Bush, C. A. (1991) *Biopolymers 31*, 1737–1746.

Prabhakaran, M. (1991) *Biochem. Biophys. Res. Commun. 178*, 192–197.

Rao, V. S. R., & Satyanarayana, B. K. (1973) *Curr. Sci. 42*, 684–685.
Rice, K. G., Weisz, O. A., Barthel, T., Lee, R. T., & Lee, Y. C. (1990) *J. Biol. Chem. 265*, 18429–18434.
Roseman, S. (1970) *Chem. Phys. Lipids 5*, 270–297.
Satyanarayana, B. K., & Rao, V. S. R. (1971) *Biopolymers 10*, 1605–1615; (1972) *Biopolymers 11*, 1115 (erratum).
Satyanarayana, B. K., & Rao, V. S. R. (1972) *Biopolymers 11*, 1379–1394.
Spiess, M. (1990) *Biochemistry 29*, 10009–10018.
Stoddart, J. F. (1971) in *Stereochemistry of Carbohydrates*, p 50, Wiley, New York.
Townsend, R. R., Hardy, M. R., Wong, T. C., & Lee, Y. C. (1986) *Biochemistry 25*, 5716–5725.
Tvaroska, I. (1991) *Curr. Opin. Struct. Biol. 2*, 661–665.
Wu, P., Rice, K. G., Brand, L., & Lee, Y. C. (1991) *Proc. Natl. Acad. Sci. U.S.A. 88*, 9355–9359.